The effect of stand homogeneity on basal area growth for unthinned and thinned Pinus taeda L. stands in southern Brazil

Ximena Mendes de Oliveira (ximena@ufra.edu.br)
Federal Rural University of the Amazon
John Paul McTague
University of Georgia
Mário Dobner Junior
Florestal Gateados
José Roberto Soares Scolforo
Federal University of Lavras, LEMAF, Campus Universitário
Henrique Ferraço Scolforo
North Carolina State University

Research Article

Keywords: Percentile method, simultaneous model, homogeneity proxy variable, Bootstrap method, initial density

Posted Date: August 9th, 2023

DOI: https://doi.org/10.21203/rs.3.rs-3225839/v1

Additional Declarations: No competing interests reported.

The effect of stand homogeneity on basal area growth for unthinned and thinned *Pinus taeda* L. stands in southern Brazil

Ximena Mendes de Oliveira[a,*], John Paul McTague[b], Mário Dobner Junior[c], José Roberto Soares Scolforo[d], Henrique Ferraço Scolforo[e]

[a,*] Federal Rural University of the Amazon, Campus Parauapebas, Department of Forest Science, Parauapebas, Pará, 68.515-000, Brazil. E-mail address: ximena@ufra.edu.br. ORCID: https://orcid.org/0000-0002-9887-7075. * Correspondent author.

[b] Warnell School of Forestry and Natural Resources, University of Georgia, Athens, GA 30603-2152, USA. E-mail address: forestbiometrician@yahoo.com. ORCID: https://orcid.org/0000-0002-0748-3637

[c] Florestal Gateados, Campo Belo do Sul, Santa Catarina 88580-000, Brazil. E-mail address: dobnerjr@gmail.com. ORCID: https://orcid.org/0000-0001-7216-781X

[d] Federal University of Lavras, LEMAF, Campus Universitário, Department of Forest Science, Campus Box 3037, Lavras, Minas Gerais 37200-000, Brazil. E-mail address: jscolforo@ufla.br. ORCID: https://orcid.org/0000-0002-5888-6751

[e] North Carolina State University, 2800 Faucette Dr., Department of Forestry and Environmental Resources, Campus Box 8001, Raleigh, NC 27695, United States. E-mail address: henriquescolforo@hotmail.com. ORCID: https://orcid.org/0000-0002-2015-5056

Authorship contribution: All authors contributed to the study conception and design. Ximena Oliveira, José Roberto Scolforo, and Henrique Scolforo: Project Idea, Processing, Analysis, Writing, Review. John Paul McTague: Analysis, Writing, Review. Mário Dobner Jr: Database, Analysis, Review.

ABSTRACT

Studies show that heterogeneity among plants interferes with stand productivity, however, this information has not been incorporated in models to assist forest managers. This paper presents a new format for growth modeling, that includes the effect of heterogeneity on final stand productivity and was developed for unthinned and thinned *Pinus taeda* stands. The data used came from a 3 x 3 factorial experiment with the factors initial density (2500, 1250, and 625 trees.ha^{-1}) and thinning (without thinning, moderate thinning, and heavy thinning). The diameter distribution represented by the percentile method were used to represent stand homogeneity. The diameters (located in the 10th and 63rd percentiles) were inserted into the basal area growth model, reducing the mean absolute error (MAE) and the square root of the mean error (RMSE) on average from 4.8433 m².ha^{-1} to 2.7702 m².ha^{-1} relative to the predicted estimates, and from 4.3139 m².ha^{-1} to 2.6984 m².ha^{-1} for the projected estimates. The validation of the equation with the homogeneity proxy variable was performed by the Bootstrap method. A simultaneous equation, compatible in prediction and projection, with the inclusion of homogeneity, is recommended for estimating the growth in the basal area of *Pinus taeda* stands in southern Brazil.

Keywords: Percentile method, simultaneous model, homogeneity proxy variable, Bootstrap method, initial density.

1. Introduction

Forest growth modeling is an important tool to assist predict, project, and simulate stand development over the years (Weiskittel et al., 2011). Such models can be grouped into different levels of resolution, such as stand-level, diameter class level, and individual tree level (Burkhart and Tomé, 2012). However, the simplicity and robustness of the stand-level model characterizes its advantages over the others. This alternative requires less information for model input and results in accurate simulations and is extensively used in forest management (Peng et al., 2000; Sun et al., 2007).

Some examples of stand models can be seen in the literature. Lam and Guan (2020) modeled stand basal area growth using a nonlinear mixed-effects model. They used data from *Cryptomeria japonica* stands at four initial densities in Taiwan. Trilleras and Aguirre (2020) compared nine basal area growth models for unthinned and thinned stands of *Eucalyptus tereticornis* in Colombia. The authors concluded that the most accurate equation for unthinned stands explained basal area as a function of age, density, and dominant height. For thinned stands, the basal area was explained by a competition index, dependent on age and dominant height of the stand.

The models represent an abstraction of the dynamics of forest stands, aiming to imitate reality (Vanclay, 1994). However, they do not consider heterogeneity. It has a direct impact on forest production. Hakamada et al. (2015) analyzed the relationship between homogeneity and productivity in clonal stands located in three states of Brazil. The study showed that heterogeneity negatively interferes with stand-level productivity. Sun et al. (2018), using data from *Sassafras tzumu* stands in China, also found a loss in stand-level productivity related to increased heterogeneity among trees.

Increased competition leads to greater growth inequality among trees, resulting in more heterogeneous stands. As resources (water, light, and nutrients) become less available, suppressed tress are less efficient in their use than dominant trees (Ryan et al., 2010). Campoe et al. (2013) observed disproportionately higher light use efficiency in 20% of the largest trees than in the 20% of the smallest trees in the stand.

Different management regimes contribute to altered competition in stands. With the removal of trees in thinning, stands tend to reduce competition and present larger trees after a certain time (McTague et al., 1989). Less dense stands also show the same described behavior (David et al., 2018). Intensive forest management can be observed in some pine stands in southern Brazil (Retslaff et al., 2016; Schneider et al., 2018; Dobner Jr. and Quadros, 2019) where the main goals are to provide products for the sawmill and pulp industry (IBÁ, 2022). Pinus is the second most planted genus in Brazil, second only to eucalyptus. More than 80% of the pine plantation areas are located in the country's southern region (IBÁ, 2022).

The study aimed to provide a new concept of integration of a proxy measure for homogeneity on forest growth, thus simulating how this silvicultural attribute reflects on stand productivity. An additional aim was to develop a simultaneous basal area growth model that considers homogeneity for *Pinus taeda* stands under different management regimes in southern Brazil.

2. Material and methods

2.1. Study area

The study area is located in Campo Belo do Sul, Santa Catarina state, southern Brazil (lat. 27°59'33"S, long. 50°54'16"W). The region presents a humid temperate climate with temperate summer (Cfb, by Köppen climate classification) and is characterized by the absence of a dry season, a maximum average temperature of 22°C in the warmest month, and an average temperature below 10°C in at least four months throughout the year (Alvares et al., 2014). Frost occurrence is frequent, ranging from two to 29 events per year (Embrapa, 1988; Dobner Jr., 2013). The altitude is approximately 1017 m above sea level, and the relief is undulated. The soils in the region are classified as Litholic Neossol, Brune Latossol, and Haplic Nitossol (Oliveira, 2012; Dobner Jr., 2013).

2.2. Characterization of the experiment

The data from *Pinus taeda* stands was conducted in a 3 x 3 factorial experiment with two repetitions (plots), implemented in 1984. The experimental factors were thinning and initial density. The plots were installed with approximately 2,000 m² in size, with a functional area of approximately 1,000 m².

The thinning factor was divided into three levels: without thinning (WT), representing the control treatment; moderate thinning (MT); and heavy thinning (HT). The initial density factor presented the levels of 2500, 1250, and 625 trees.ha^{-1}; thus, the experiment comprises nine treatments arising from the combination between the factors, and eighteen plots, since each treatment has two repetitions (Figure 1).

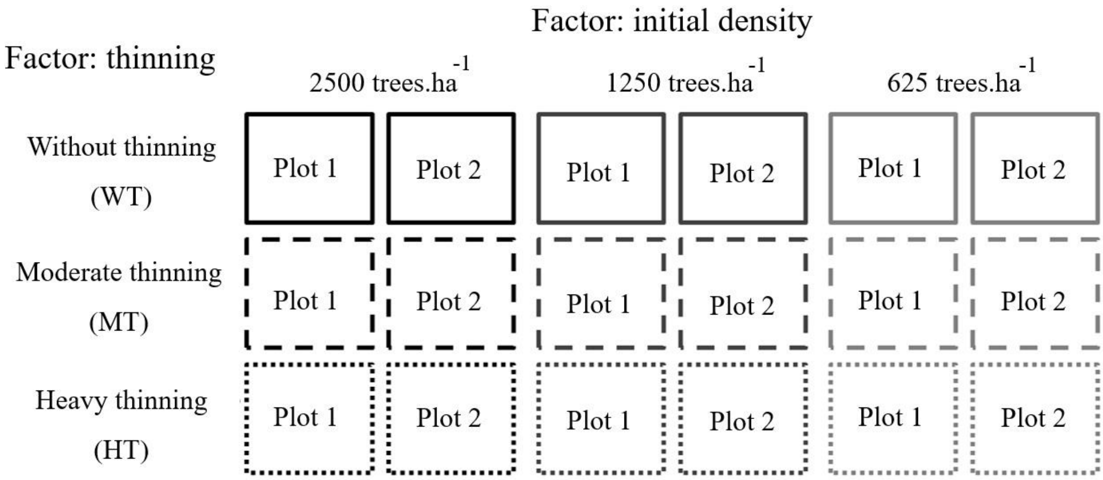

Fig 1 - Experiment in a 3 x 3 factorial scheme with two repetitions with the factors thinning and initial density.

Table 1 shows the tree removal percentage in each treatment, calculated by the ratio between the trees removed in each thinning and the initial density multiplied by 100.

Table 1 - Percentage of tree removal, over the years, in the six treatments that had thinning from above.

Treatment	Plot	Age (years)				Total
		5	8	12	27	
MT x 2500 $trees.ha^{-1}$	1	18 %	16 %	11 %	6 %	51 %
	2	16 %	14 %	13 %	5 %	48 %
MT x 1250 $trees.ha^{-1}$	1	-	24 %	22 %	11 %	57 %
	2	-	30 %	14 %	8 %	52 %
MT x 625 $trees.ha^{-1}$	1	-	26 %	19 %	11 %	56 %
	2	-	31 %	25 %	8 %	64 %
HT x 2500 $trees.ha^{-1}$	1	30 %	20 %	17 %	8 %	75 %
	2	35 %	15 %	9 %	12 %	71 %
HT x 1250 $trees.ha^{-1}$	1	-	58 %	11 %	10 %	79 %
	2	-	54 %	10 %	11 %	75 %
HT x 625 $trees.ha^{-1}$	1	-	66 %	-	9 %	75 %
	2	-	67 %	-	7 %	74 %

The thinning used in the experiment followed the methodology of "crown thinning" (Dobner Jr., 2015), in which 400 $trees.ha^{-1}$ in each plot were selected as potential trees (dominant individuals, of good quality and homogeneously distributed in the stand) in the first stage (Figure 2a). Then, competing trees (well-developed individuals that, for some reason, were not selected as potential trees) were selected (Figure 2b) and removed (Figure 2c), providing significant openings in the stand canopy for the remaining trees to develop. Pruning was performed only in the treatments with thinning, as follows:

pruning all trees up to 2.5 m tall at five years of age and pruning only selected potential trees up to 6 m tall at seven years.

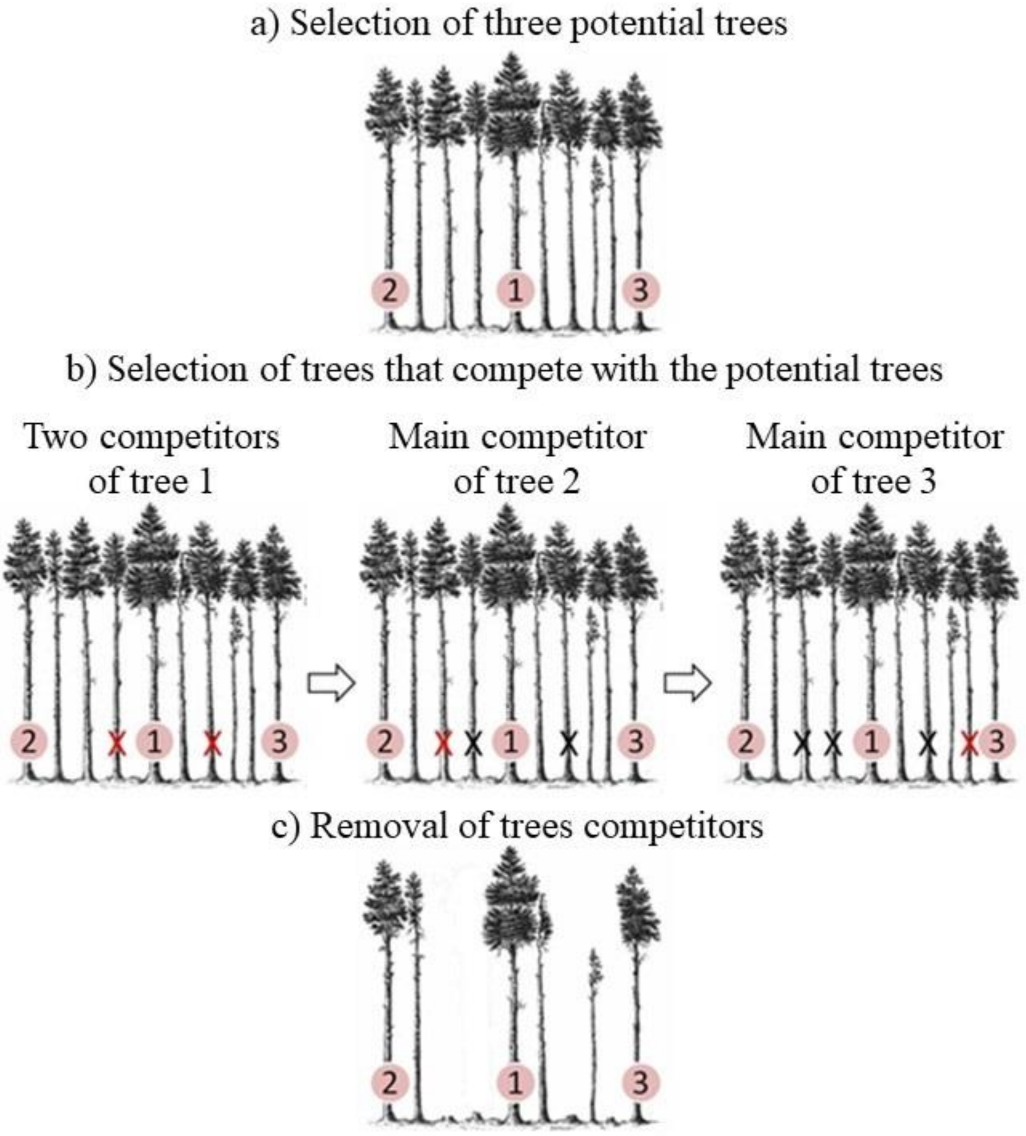

Fig 2 - Description of the steps considered in the crown thinning methodology.

2.3. Data characterization

The diameter at 1.3 m (dbh) of all trees in the plots were measured from 5 to 33 years of age. The collection was done annually in the interval between 5 and 17 years. After that, the collection was performed at 19, 27, 30, 31, 32, and 33 years of age. The dominant height (H) of the plots was obtained by considering the average height of the 100 trees with the highest dbh per hectare (Assmann, 1970).

The description of the data, considering the nine treatments, is shown in Table 2.

Table 2 - Minimum, maximum, average, and standard deviation of variables obtained in unthinned and thinned *Pinus taeda* stands.

Variable	Minimum	Maximum	Average	Standard Deviation
dbh (cm)	1.5	74.0	23.8	10.3
H (m)	6.0	31.6	19.4	8.0
B (m^2. ha^{-1})	7.8	93.9	42.8	17.2
N ($trees.ha^{-1}$)	126	2512	819	561
A (years)	5	33	16	9

dbh is the diameter at 1.3 m of the trees; H is the dominant height in the plot at each age, that considers the average height of the 100 largest diameter stems/ha; B is the basal area in the plot at each age; N is the number of $trees.ha^{-1}$ in the plot at each age; A is the age.

2.4. Simultaneous basal area prediction and projection

The basal area model follows Schumacher's baseline model, in which the basal area is estimated as a function of age, dominant height, stand density, and thinning intensity, according to expression (1):

$$\ln(B) = \beta_0 + \beta_1 \frac{1}{A} + \beta_2 \ln(H) + \beta_3 \ln(N) + \beta_4 \frac{N_t A_t}{A N_a} \quad (1)$$

where $\beta_{i's}$ β_i are the model parameters; N_t is the number of trees removed in the last thinning; N_a is the number of trees remaining after the last thinning; A_t is the age at the last thinning. Other variables have been described previously.

The thinning index ($(N_t A_t)/(AN_a)$), proposed by Pienaar and Shiver (1986) allows the model to be used in unthinned and thinned stands over a wide range of values for age, site quality, density, and thinning intensity. This index considers simulated rates of percent removal of individuals at different ages, the impact that will be caused in basal area removal, and the growth that will occur after this intervention.

From this base model used in the prediction, it is possible to impose algebraic restrictions to obtain the projection model in polymorphic form. By considering the conditions that $B = B_1$ at age 1 (A_1) and $B = B_2$ at age 2 (A_2) and isolating the term β_1, it is possible to obtain the projection model in the polymorphic form (2):

$$\ln(B_2) = \frac{A_1}{A_2}\ln(B_1) + \beta_1\left(1 - \frac{A_1}{A_2}\right) + \beta_2\left[\ln(H_2) - \frac{A_1}{A_2}\ln(H_1)\right] + \beta_3\left[\ln(N_2) - \frac{A_1}{A_2}\ln(N_1)\right] + \beta_4\left[\frac{N_t A_t}{A_2 N_a} - \frac{A_1}{A_2}\frac{N_t A_t}{A_1 N_a}\right] \quad (2)$$

where B_2 is the projected basal area ($m^2.ha^{-1}$) for future age (A_2); B_1 is the basal area ($m^2.ha^{-1}$) at the current age (A_1); H_2 is the dominant height at the age A_2; H_1 is the dominant height at the age A_1; N_2 is the number of individuals at the age A_2; N_1 is the number of individuals at the age A_1; N_t is the number of trees removed in the last thinning; N_a is the number of trees remaining after the last thinning; A_t is the age of the last thinning. Other variables have been described previously.

The simultaneous fitting technique used to ensure compatibility between the basal area prediction and projection model was presented by McTague et al. (2008) and Scolforo et al. (2019b). In this technique, all forward combinations of plot remeasurements for each plot were combined in the fitting dataset, helping to model asymptotic behavior more reliably. A plot with three measurement ages, for example, has three pairings (ages 1 and 2, 1 and 3, and 2 and 3). To exemplify the matrix form (3), the prediction (1) and projection models in the polymorphic form (2) were considered at three age intervals:

$$Y = \alpha_0 X_1 + \alpha_1 X_2 + \alpha_2 X_3 + \alpha_3 X_4 + \alpha_4 X_5 \qquad (3)$$

$$
\begin{array}{c} Y \\ \left| \begin{array}{c}
ln(B_{11}) \\
ln(B_{12}) \\
ln(B_{13}) \\
ln(B_{12}) - \frac{A_{11}}{A_{12}} ln(B_{11}) \\
ln(B_{13}) - \frac{A_{11}}{A_{13}} ln(B_{11}) \\
ln(B_{13}) - \frac{A_{12}}{A_{13}} ln(B_{12})
\end{array} \right| \end{array}
=
\begin{array}{ccccc} X_1 & X_2 & X_3 & X_4 & X_5 \\ \end{array}
\left| \begin{array}{ccccc}
1 & \frac{1}{A_{11}} & ln(H_{11}) & ln(N_{11}) & \frac{N_t A_t}{A_{11} N_a} \\
1 & \frac{1}{A_{12}} & ln(H_{12}) & ln(N_{12}) & \frac{N_t A_t}{A_{12} N_a} \\
1 & \frac{1}{A_{13}} & ln(H_{13}) & ln(N_{13}) & \frac{N_t A_t}{A_{13} N_a} \\
0 & 1 - \frac{A_{11}}{A_{12}} & ln(H_{12}) - \frac{A_{11}}{A_{12}} ln(H_{11}) & ln(N_{12}) - \frac{A_{11}}{A_{12}} ln(N_{11}) & \frac{N_t A_t}{A_{12} N_a} - \frac{A_{11}}{A_{12}} \frac{N_t A_t}{A_{11} N_a} \\
0 & 1 - \frac{A_{11}}{A_{13}} & ln(H_{13}) - \frac{A_{11}}{A_{13}} ln(H_{11}) & ln(N_{13}) - \frac{A_{11}}{A_{13}} ln(N_{11}) & \frac{N_t A_t}{A_{13} N_a} - \frac{A_{11}}{A_{13}} \frac{N_t A_t}{A_{11} N_a} \\
0 & 1 - \frac{A_{12}}{A_{13}} & ln(H_{13}) - \frac{A_{12}}{A_{13}} ln(H_{12}) & ln(N_{13}) - \frac{A_{12}}{A_{13}} ln(N_{12}) & \frac{N_t A_t}{A_{13} N_a} - \frac{A_{12}}{A_{13}} \frac{N_t A_t}{A_{12} N_a}
\end{array} \right|
*
\begin{array}{c} \alpha \\ \left| \begin{array}{c}
\alpha_0 \\ \alpha_1 \\ \alpha_2 \\ \alpha_3 \\ \alpha_4
\end{array} \right| \end{array}
$$

where, indices 11, 12 and 13 refers to plot 1 and the ages of the plot measurement; other variables are previously defined.

2.4.1 Simultaneous prediction and projection of basal area and incorporating the effect of plantation homogeneity

Homogeneity is directly related to the productivity of a stand; thus, an increase in inequality among trees, as expressed by a wider diameter distribution, is associated with a reduced growth rate (Sun et al. 2018). Heterogeneous stands have a greater number of suppressed trees that are more likely to die over time compared to larger trees (Binkley et al., 2003).

According to McTague and Bailey (1987), the diameter distribution can identify different growth rates between plots. The narrower and higher the curve of the diameter distribution, the more homogeneous the plot is, and under these conditions, the more accelerated the growth is. The authors also state that the diameters located in the 10th (d10) and 63rd (d63) percentiles are far enough apart to provide the distribution range and can serve to identify heterogeneity in forest growth. It should be noted that the exact percentile used is 63.21, however d63 is a convenient label for the 63rd diameter percentile. The 63rd diameter percentile implies that 63% of the trees in the stand have that diameter or less.

Commonly adopted approaches to basal area growth modeling assume that stands with the same basal area at age 1, same site quality, and same density will grow identically. However, Figure 3 provides an example of why this is not necessarily true for *Pinus taeda* stands.

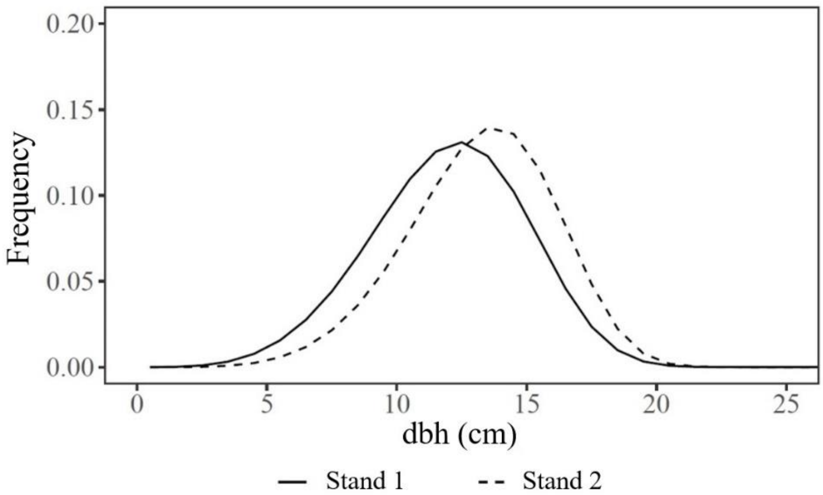

Fig 3 - Diameter distribution in *Pinus taeda* stands with the same density, dominant height, and basal area.

Information about the distributions was considered by including the diameter percentiles d10 and d63 in the model to reflect plot homogeneity. The diameter distributions resulting from these percentiles were related to the uniformity index PB50. This index was proposed with the same methodology used in the PV50 (Hakamada et al., 2015); however, the variable considered was the basal area of the stand and not the stand volume. Thus, modeling the percentiles is simpler than modeling the uniformity index. The model with the percentiles incorporates the effect of homogeneity in three steps:

In the first step, the diameter percentile d10 was entered into the basal area prediction (1) and projection (2) models. This percentile is located in the midst of the suppressed trees. The inclusion resulted in the following set of prediction (4) and projection (5) models:

$$\ln(B) = \beta_0 + \beta_1 \frac{1}{A} + \beta_2 \ln(H) + \beta_3 \ln(N) + \beta_4 \frac{N_t A_t}{A N_a} + \beta_5 \ln(d10) \tag{4}$$

$$\ln(B_2) = \frac{A_1}{A_2}\ln(B_1) + \beta_1\left(1 - \frac{A_1}{A_2}\right) + \beta_2\left[\ln(H_2) - \frac{A_1}{A_2}\ln(H_1)\right] + \beta_3\left[\ln(N_2) - \frac{A_1}{A_2}\ln(N_1)\right] + \beta_4\left[\frac{N_t A_t}{A_2 N_a} - \frac{A_1}{A_2}\frac{N_t A_t}{A_1 N_a}\right] + \beta_5\left[\ln(d10_2) - \frac{A_1}{A_2}\ln(d10_1)\right] \tag{5}$$

where $d10_2$ is the diameter at the 10th percentile (cm) at the future age (A_2); $d10_1$ is the diameter at the 10th percentile (cm) at the current age (A_1). Other variables have been described previously.

The second step obtains an estimate of d10 using a recursive system of equations involving higher diameter percentile, namely d63. The prediction model (6) imposed algebraic restrictions on current and future age, and the term β_0 was isolated, generating the projection model in anamorphic form (7).

$$\ln(d10) = \beta_0 + \beta_1 \ln(d63) + \beta_2 \ln(N) \tag{6}$$

$$\ln(d10_2) = \ln(d10_1) + \beta_1[\ln(d63_2) - \ln(d63_1)] + \beta_2[\ln(N_2) - \ln(N_1)] \tag{7}$$

where $d63_2$ is the diameter at the 63rd percentile (cm) at the future age (A_2); $d63_1$ is the diameter at the 63rd percentile (cm) at the current age (A_1). Other variables have been described previously.

Finally, the third step obtains an estimate of the 63rd diameter percentile, d63. Information on thinning was considered in this step and therefore implicitly is included in the set of models to obtain d10. The prediction model (8) and the projection model in anamorphic form (9) are shown below:

$$\ln(d63) = \beta_0 + \beta_1 \ln(H) + \beta_2 \ln\left(\frac{A}{N}\right) + \beta_3 \frac{N_t A_t}{\mathrm{A} N_a} \tag{8}$$

$$\ln(d63_2) = \ln(d63_1) + \beta_1[\ln(H_2) - \ln(H_1)] + \beta_2\left[\ln\left(\frac{A_2}{N_2}\right) - \ln\left(\frac{A_1}{N_1}\right)\right] + \beta_3\left(\frac{N_t A_t}{\mathrm{A}_2 N_a} - \frac{N_t A_t}{\mathrm{A}_1 N_a}\right) \tag{9}$$

2.5 Evaluating the Accuracy of Models

Processing was performed in the R software (R Core Team, 2019). Graphs were generated using the ggplot2 package (Wickham, 2016).

Akaike's information criterion (AIC) and Bayesian information criterion (BIC) were used to evaluate the performance of the adjusted models. The statistics of mean error (T), mean absolute error (MAE), and root mean square error (RMSE), Eqs. (10 - 12) were used to evaluate the estimates related to the prediction and projection of the simultaneous models. Additionally, graphs were generated to analyze the estimates' behavior.

$$T = \frac{1}{n}\sum_{i=1}^{n}(O - \mathrm{P}) \tag{10}$$

$$MAE = \frac{1}{n}\sum_{i=1}^{n}|O - P| \tag{11}$$

$$RMSE = \sqrt{\frac{\sum_{i=1}^{n}(O - \mathrm{P})^2}{n}} \tag{12}$$

i is the number of observations ranging from 1 to n; O are the observed values, and P are the predicted values. Other variables have been described previously.

The estimates' validation related to the basal area model projection with the insertion of a proxy homogeneity variable was performed by the non-parametric Bootstrap method with replacement (Efron, 1982), considering a total of 100 random samples. These random samples allowed estimating the sample distribution of the statistics (T, MAE, and RMSE) and generating quality measures of the statistical fit. This technique has been used in other studies to enable validation (Scolforo et al., 2018; Hall et al., 2019; Santos et al., 2021).

3. Results

3.1. Behavior of the stand homogeneity proxy variable

As McTague and Bailey (1987) discussed, the shape of the diameter distribution can express the homogeneity among trees located in different plots. The leptokurtic form of the distribution (high and narrow curve) characterizes a stand with less competition and faster tree growth. In this condition, the trees tend to present less variation in size, resulting in a more homogeneous population. From the moment the curve is altered to mesokurtic and platykurtic forms with height reduction and increase in width, the stand is in a condition of greater competition; therefore, the trees present more limited growth. Under this condition, the trees tend to grow more unevenly, and the variation in tree size increases.

Figure 4 allows for the evaluation of the homogeneity effect in the population at four distinct moments: a) age five, before thinning to evaluate the behavior under identical conditions within each initial density; b) at ten years, because this is the moment when the trees are in a high rate of inter-tree competition at the initial densities of 2500 and 1250 trees.ha^{-1}; c) at 19 years; and d) at 30 years because this is when all thinning has already been performed.

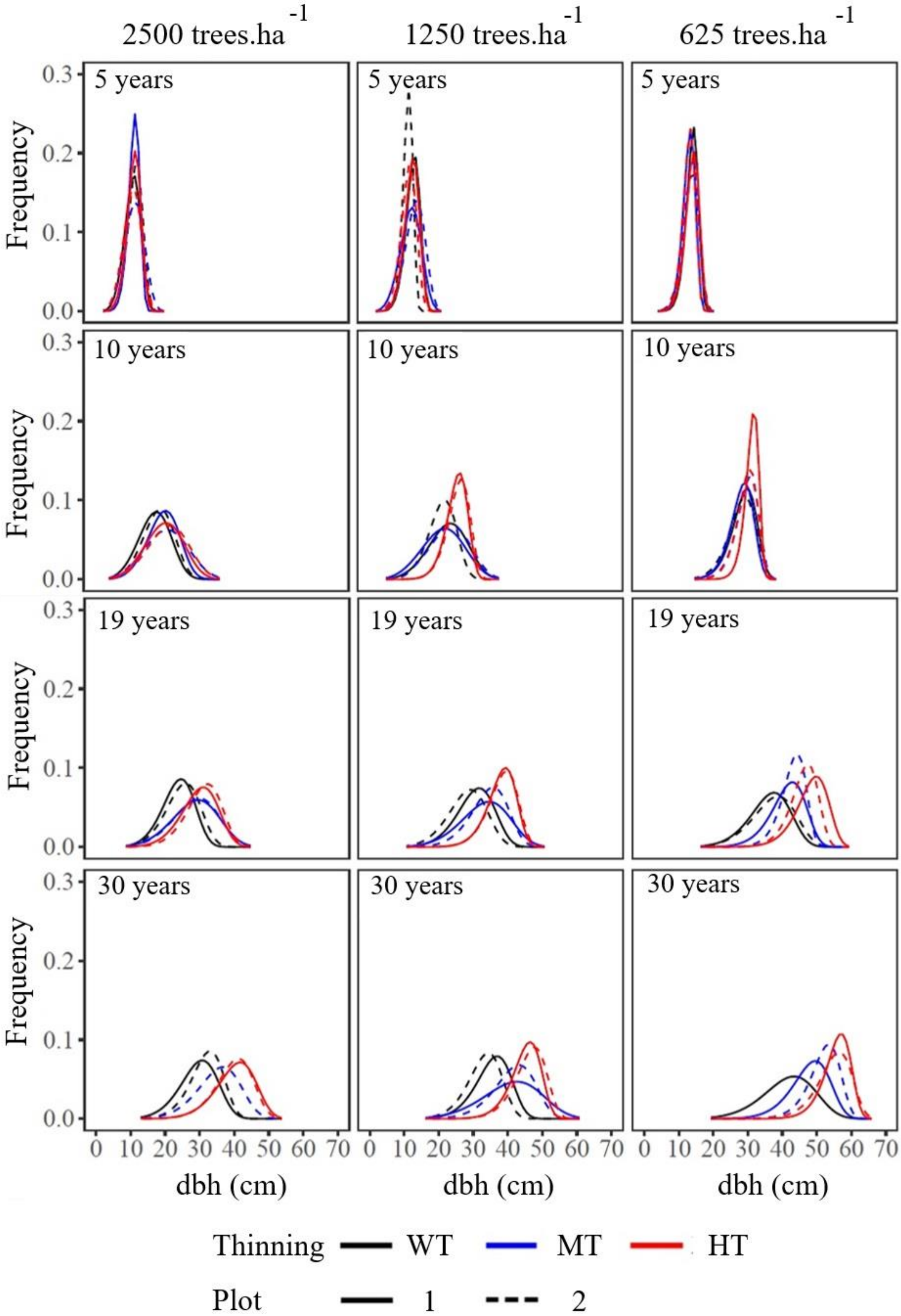

Fig 4 - Two-parameter Weibull diameter distribution with parameters recovered by the percentile method with diameters at the 10th and 63rd percentiles at ages 5, 10, 19, and 30 years.

All the plots showed narrow and high curves at age 5, indicating accelerated growth and greater homogeneity. It is only possible to observe the initial density effect at this age because no plot has been thinned yet. The plots in stands with medium and high initial density showed greater spread than the plots in the stand with lower initial density, where the trees have more space to develop.

The curves became wider and flatter at ten years and have shifted to the right, as a result of tree growth. At an initial density of 2500 trees.ha^{-1}, the competition remained intense, with or without thinning. For treatments with medium and low initial density, the thinning effect is already seen in the HT factor, which showed greater residual tree growth indicated by the curve height and shift to the right.

At 19 years of age, at an initial density of 2500 trees.ha^{-1}, the curves showed similar heights, but the thinned plots were positioned more to the right, indicating the presence of larger trees than the WT plots. In plots with an initial density of 1250 and 625 trees.ha^{-1}, the HT plots showed faster growth and larger trees, followed by the MT and WT plots.

Finally, at 30 years of age, all plots were analyzed for initial density and response to thinning. Plots submitted to HT showed larger trees at the three initial densities. At 1250 and 625 trees.ha^{-1}, the HT treatment showed greater homogeneity with higher and narrower curves. Plots subjected to MT showed intermediate tree size at the three initial densities. At the initial density of 625 trees.ha^{-1}, the MT treatment distribution display greater homogeneity, with higher and narrower curves than plots that did not undergo thinning. The plots without thinning (WT) display smaller trees at the three initial densities and generally greater heterogeneity.

Thus, a strong relationship was observed between production and diameter distributions because lower initial densities and higher thinning intensities favored greater stand homogeneity and higher tree growth rates. Although thinning from above could theoretically increase heterogeneity by removing well-developed trees, the removal of some trees forestalls mortality and favors stand homogeneity.

3.2. Simultaneous basal area modeling

Since the curves of the diameter distributions can express the homogeneity of the plots (Figure 4), the use of the diameters located in the 10^{th} and 63^{rd} percentiles was considered in the development of a simultaneous prediction and projection stand-level basal area model.

The equations that considered the homogeneity of the plots (4 and 5) at different ages showed more accurate behavior than equations 1 and 2, that did not include a homogeneity proxy variable. (Figure 5). The equations presented significant coefficients (for α=0.05) with algebraic signs suitable for describing biological behavior of stand growth, and the AIC and BIC values reduced dramatically with the insertion of homogeneity, indicating model improvement (Table 3).

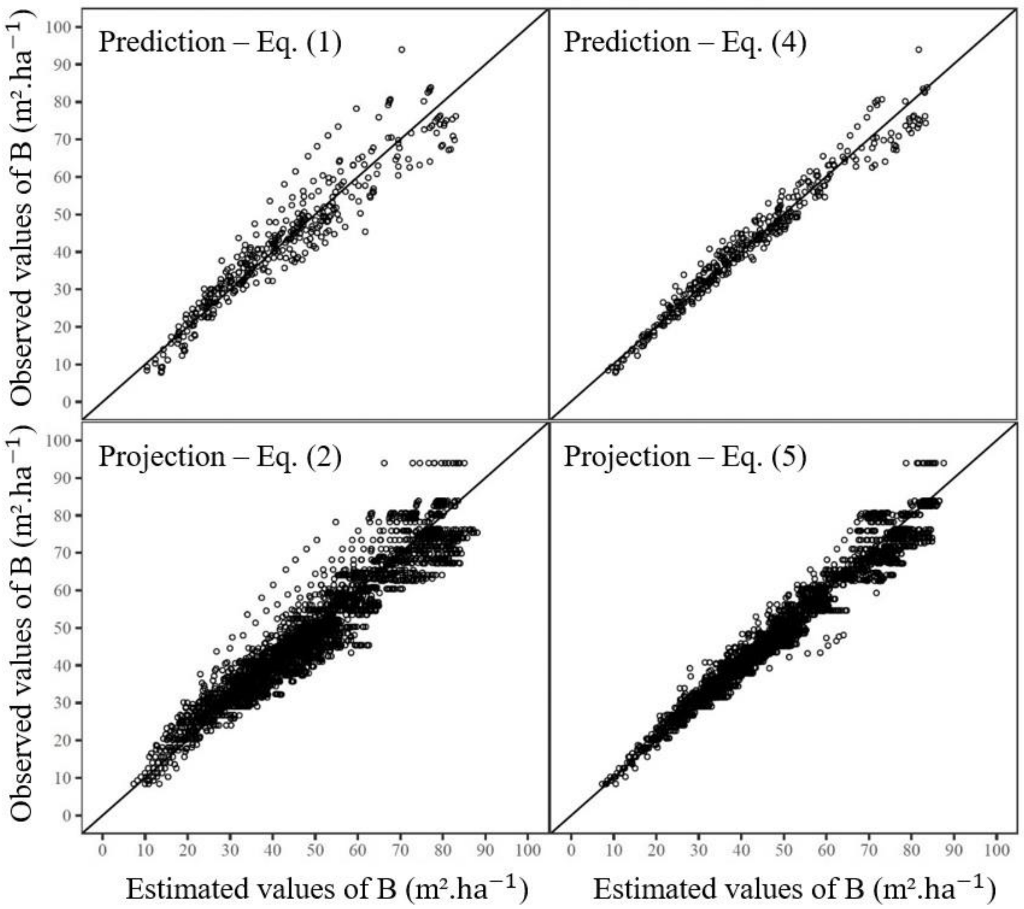

Fig 5 - Behavior of estimated values with respect to observed values in the prediction and projection of the basal area in the simultaneous model without the homogeneity proxy variable (Eqs. 1 and 2) and with the homogeneity proxy variable (Eqs. 4 and 5).

Table 3 - Simultaneous prediction and projection models in basal area, estimated values (EV) of the coefficients with their respective standard errors (SE), and fit statistics (AIC and BIC).

Simultaneous Model	Coefficients	EV	SE	AIC	BIC
Basal area model	β_0	-1.5564	0.0408	-6461.612	-6423.718
(Eqs. 1 and 2)	β_1	-1.5585	0.0471		
	β_2	0.8645	0.0086		
	β_3	0.4503	0.0050		
	β_4	-0.1453	0.0064		
Basal area model with	β_0	-4.2240	0.0441	-10030.190	-9985.983
homogeneity proxy	β_1	-4.2461	0.0469		
variable	β_2	0.1708	0.0108		
(Eqs. 4 and 5)	β_3	0.7791	0.0054		
	β_4	-0.1084	0.0042		
	β_5	0.9041	0.0120		

The models used to predict and project d10 (6 and 7) and d63 (8 and 9) were fit with results presented in Table 4. The coefficients were significant, considering α=0.05, and presented low values in the fit statistics (AIC and BIC). The relationship between estimated and observed values for the two simultaneous models is represented in Figure 6.

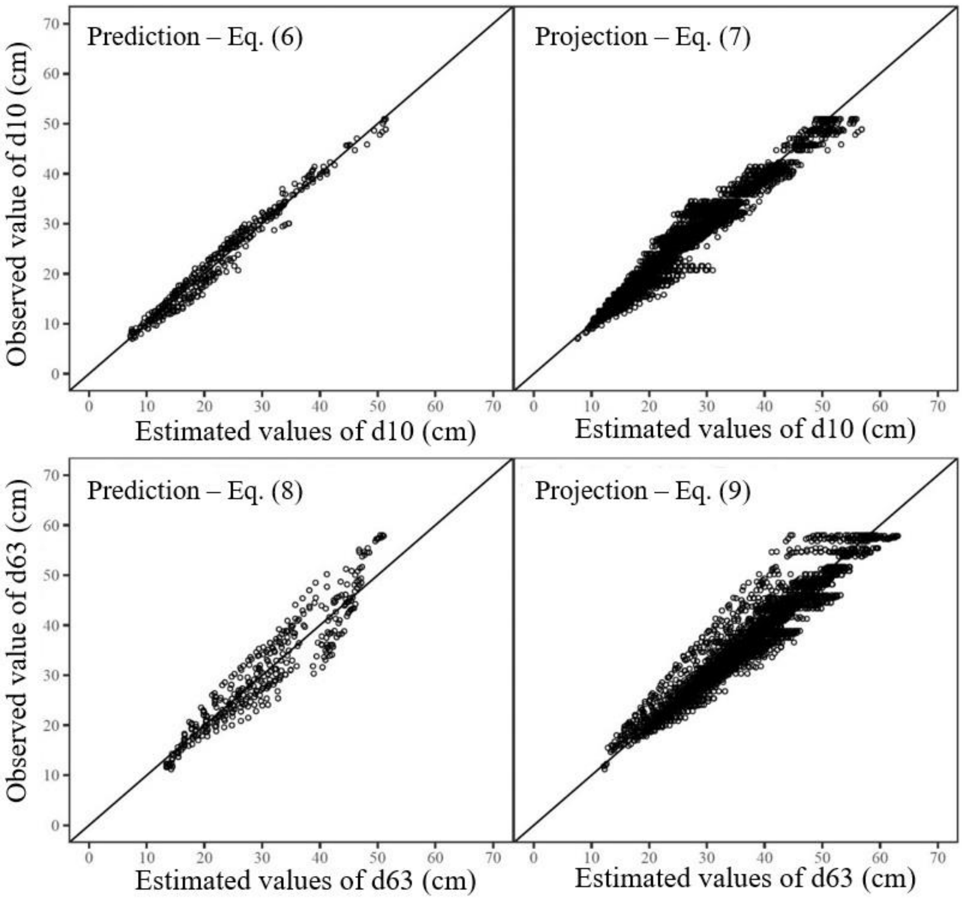

Fig 6 - estimated and observed values in the prediction and projection of the diameters at the 10th (Eqs. 6 and 7) and 63rd (Eqs. 8 and 9) percentiles.

Table 4 - Simultaneous prediction and projection models of the 10th and 63rd diameter percentiles, estimated values (EV) of the coefficients with their respective standard errors (SE), and fit statistics (AIC and BIC).

Simultaneous Model	Coefficients	EV	SE	AIC	BIC
d10 model	β_0	0.9494	0.0428	-9147.145	-9121.882
(Eqs. 6 and 7)	β_1	0.9283	0.0052		
	β_2	-0.1604	0.0041		
d63 model	β_0	2.2497	0.0320	-9058.812	-9027.233
(Eqs. 8 and 9)	β_1	0.5251	0.0067		
	β_2	0.1018	0.0033		
	β_3	0.0191	0.0033		

3.3. Estimation of the traditional basal area model versus the enhanced basal area model with the homogeneity proxy variable

The accumulated or propagated error of the models was included in the model with the homogeneity proxy variable, that is, the estimated $d63_2$ was used to obtain the estimated $d10_2$, and both were considered implicitly and explicitly for the estimates of stand basal area (B_2). Even with the insertion of more models (and their respective propagated errors), the quality of the basal area estimates improved with the homogeneity proxy variable (Table 5).

Table 5 - T, MAE, and RMSE statistics used to assess the estimates of the simultaneous models for the basal area and the 10th and 63rd diameter percentiles. Eqs. (1) and (2) do not have propagated errors for basal area, however they omit the percentile variables and estimate of homogeneity. Eqs. (4) and (5) utilize the predicted and projection diameter percentile values of Eqs. (6-9) and do contain propagated errors.

Simultaneous basal area model	Prediction Statistics			Projection statistics		
	T ($m^2.ha^{-1}$)	MAE ($m^2.ha^{-1}$)	RMSE ($m^2.ha^{-1}$)	T ($m^2.ha^{-1}$)	MAE ($m^2.ha^{-1}$)	RMSE ($m^2.ha^{-1}$)
Eqs. 1 and 2	0.2371	4.1120	5.5746	-0.3749	3.6495	4.9782
Eqs. 4 and 5	0.2459	2.3346	3.2057	0.1752	2.2310	3.1657
Simultaneous model of d10 and d63	Prediction Statistics			Projection statistics		
	T (cm)	MAE (cm)	RMSE (cm)	T (cm)	MAE (cm)	RMSE (cm)
Eqs. 6 and 7	0.4689	2.6133	3.1562	-0.1117	2.1126	3.0959
Eqs. 8 and 9	0.3365	2.9360	3.6685	-0.2582	1.8903	2.8706

As the model with the homogeneity proxy variable obtained the best results, 100 samples were randomized by the non-parametric Bootstrap method with replacement to check if, at some point, the accuracy of the new model would worsen. These random samples allowed estimating the sample distribution of the T, MAE, and RMSE statistics (Table 6, Figure 7). The model showed high accuracy and low bias associated with the projected estimates. Confidence intervals with a 95% level exhibited short lengths, which reinforced the accuracy of the projected basal area values.

Table 6 - Validation statistics (T, MAE, and RMSE) and their confidence intervals (95 %) on plot basal area projection.

Statistics	Mean	Confidence Interval (95%)	
		Lower Limit	Upper Limit
T ($m^2.ha^{-1}$)	-0.1663	-0.3016	-0.0469
MAE ($m^2.ha^{-1}$)	2.3620	2.2580	2.4530
RMSE ($m^2.ha^{-1}$)	3.4430	3.2110	3.6930

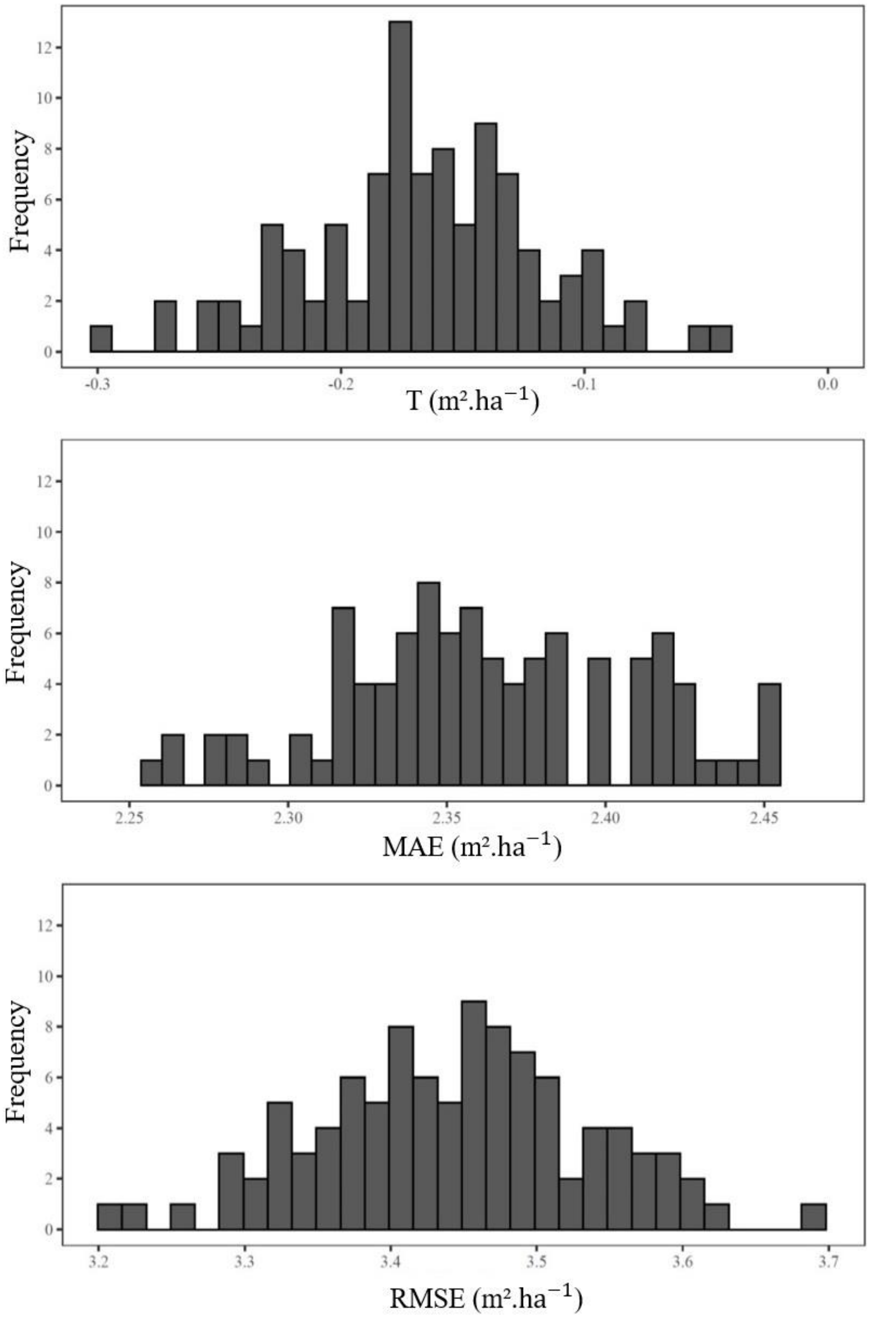

Fig 7 - Sample distribution of the validation statistics (T, MAE, and RMSE) calculated for the 100 samples randomized by the non-parametric Bootstrap method with replacement.

3.4. Growth curves considering different planting homogeneities

Two plots of the treatment with an initial density of 625 trees.ha^{-1} and moderate thinning and two plots of the treatment with an initial density of 1250 trees.ha^{-1} and heavy thinning were used for demonstration. Homogeneous stands showed greater growth than heterogeneous stands in the two situations shown (Figure 8). The growth of the stand basal area from the same site, density, thinning, and age demonstrates different behaviors, in accordance with the diameter distribution. Thus, the importance of the homogeneity proxy variable ensures flexibility of the model and improvement of the estimate.

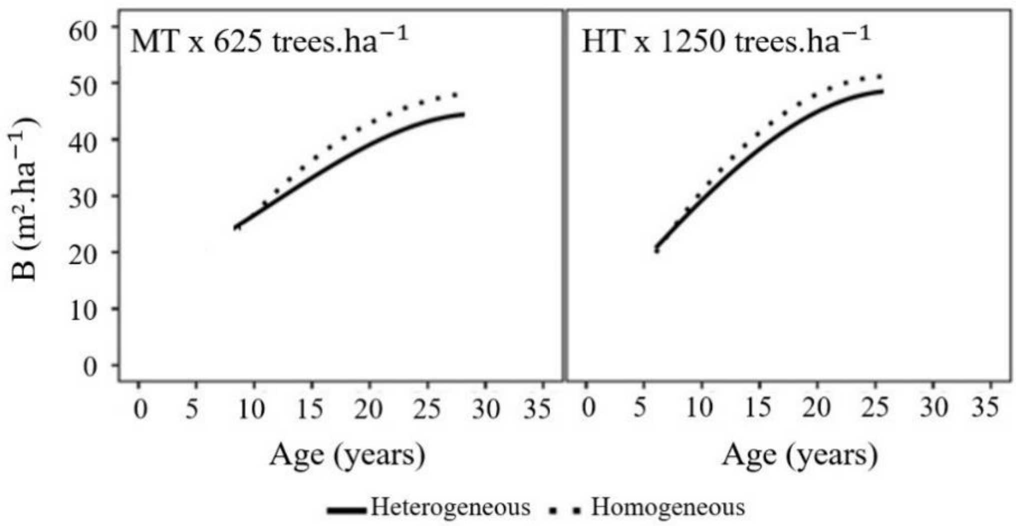

Fig 8 - Basal area curves generated for homogeneous and heterogeneous stands.

4. Discussion

Forest growth and production models are important in forest management planning (Weiskittel et al., 2011). We propose the inclusion of homogeneity as a variable and demonstrate its impact on future stand growth. Montes (2012) considered temperature variation to explain the growth in *Pinus taeda* stands in the southern United States. Scolforo et al. (2019b) included a water availability factor in a growth and production system composition. The authors used data from eucalypt stands with clones belonging to four genetic families planted in different regions of Brazil. This study included the effect of silvicultural quality (stand homogeneity) in the model. Although silvicultural quality also greatly impacts growth, models that quantify this effect are lacking.

Hakamada et al. (2015) and Sun et al. (2018) found that more homogeneous stands show higher stand-level productivity than less homogeneous ones.

Initial density and thinning intensity alter the growth rates of trees in the stand and the size of individual trees (David et al., 2018; Dobner Jr. and Quadros, 2019; Lam and Guan, 2020). Ryan et al. (2010) found that increased competition between trees causes lower resource use efficiency (water, light, and nutrients) by suppressed individuals. Campoe et al. (2013) observed higher light use efficiency of the 20% largest trees compared to the 20% smallest trees in the stand. Binkley et al. (2003) found a slower growth rate of suppressed trees than dominant trees. Thus, increased competition causes greater growth inequality among trees, resulting in more heterogeneous stands.

Similar to the observations in this study, Sun et al. (2018) found an increase in heterogeneity with increasing stand age, so that the higher the initial density, the more pronounced was the inequality among trees until the onset of self-thinning when homogeneity slowly re-established. The authors also found that regardless of age, site, initial density, and thinning, increased inequality in tree size was always associated with lower productivity at the stand-level. Thus, the thinning methodology applied in this study (Dobner Jr., 2015) efficiently reduced competition between trees and provided greater plot homogeneity over time and a higher growth rate than the rate of an unthinned treatment.

The diameters located in the 10^{th} and 63^{rd} percentiles express the distribution range and homogeneity of the stand (McTague and Bailey, 1987). The explicit (d10) and implicit (d63) addition of diameters in the simultaneous basal area growth model resulted in better estimates and flexibility. McTague and Bailey (1987) did not obtain precise information on thinning amount and intensity in their database; however, they could develop a simple and robust model with diameters percentiles. Scolforo et al. (2019a) developed a forest growth and production system linking the stand and individual tree levels using diameters at different percentiles.

After the regression fit, model validation is an important process in developing a supervised model, and the non-parametric Bootstrap method with replacement is one of the viable alternatives to perform this procedure. The larger the randomized sample amount, the better the approach, as the models approximate the central limit theory for the simulated dataset (Xu and Goodacre, 2018). Scolforo et al. (2018) used this methodology to validate a generalized thinning model, and Hall et al. (2019) used this methodology to validate a forest growth and production system. In this study, 100 samples were randomized and showed accurate T, MAE, and RMSE statistics.

Future studies can be conducted using other species and different regions. The equation obtained in this study is appropriate for *Pinus taeda* stands in southern Brazil, with different initial densities and thinning intensities.

5. Conclusion

Stand homogeneity is related to a higher growth rate of trees and is affected by initial density and thinning over time. Higher initial densities lead to greater heterogeneity and a lower growth rate than lower densities. Thinning was efficient in increasing the homogeneity and growth rate of residual trees; therefore, the higher the removal intensity, the more efficient it was in terms of homogeneity.

The methodology developed considered the stand homogeneity through the diameter's explicit insertion at the 10th percentile and implicitly with the diameter's recursive system at the 63rd percentile in the simultaneous model (prediction and projection) of the basal area at the stand-level. The information on the diameters in these percentiles is available from data collected in the forest inventory, and does not require an extra cost for collecting this information in the field.

The resulting system of equations can generate current and future estimates of the basal area at the stand-level in *Pinus taeda* plantations that are unthinned and thinned at different intensities using the crown thinning methodology in southern Brazil. The methodological approach developed can be extrapolated and implemented using other species and management alternatives.

The gain in model flexibility at the stand-level was the focus of this study. From these estimates, information at the level of diameter classes and individual trees can be disaggregated, bringing more detailed information for management aiming to obtain wood of larger dimensions.

Acknowledgments

The authors are especially grateful to the private enterprise Florestal Gateados, Forest Management Laboratory (LEMAF) ate Federal University of Lavras (UFLA) and Coordenação de Aperfeiçoamento de Pessoal de Nível Superior (CAPES).

Declaration of Competing Interest

The authors declare that they have no known competing financial interests or personal relationships that could have appeared to influence the work reported in this paper. The authors did not receive support from any organization for the submitted work.

References

Alvares CA, Stape JL, Sentelhas PC, Gonçalves JLM, Sparovek G (2013) Köppen's climate classification map for Brazil. Meteorol. Zeitschrift 22:711–728. https://doi.org/10.1127/0941-2948/2013/0507

Assmann E (1970) The principles of forest yield study. Oxford: Pergamon Press

Binkley D, Senock R, Bird S, Cole TG (2003) Twenty years of stand development in pure and mixed stands of *Eucalyptus saligna* and nitrogen-fixing *Facaltaria moluccana*. For. Ecol. Manage. 182(1–3):93–102. https://doi.org/10.1016/S0378-1127(03)00028-8

Burkhart HE, Tomé M (2012) Modeling Forest Trees and Stands. Springer, New York

Campoe OC, Stape JL, Nouvellon Y, Laclau JP, Bauerle WL, Binkley D, Le Maire G (2013) Stem production, light absorption and light use efficiency between dominant and non-dominant trees of *Eucalyptus grandis* across a productivity gradient in Brazil. For. Ecol. Manage. 288:14–20. https://doi.org/1016/j.foreco.2012.07.035

David HC, Péllico Netto S, Arce JE, Woycikievicz APF, Araújo EJG, Miranda ROV (2018) Intensive management for optimizing the production of high-value logs of pine forests in southern Brazil. Ci. Fl. 28 (3): 1303-1316. https://doi.org/10.5902/1980509833352

Dobner Jr M (2013) Crown thinning effects on growth and wood quality of *Pinus taeda* stands in southern Brazil. PhD Thesis, Albert-Ludwigs-Universität

Dobner Jr. M. (2015) Desbaste pelo alto: uma alternativa rentável para povoamentos de *Pinus taeda* no Sul do Brasil. Santa Catarina State, Brazil.

https://engenhariaflorestal.paginas.ufsc.br/files/2015/09/Cartilha_desbaste_Dobner-e-Huss.pdf Acessed 25 April 2022

Dobner Jr. M, Quadros DS (2019) Economic performance of loblolly pine stands in southern Brazil as a result of different crown thinning intensities. Rev. Árvore 43(2):1-11. https://doi.org/10.1590/1806-90882019000200004

Efron B (1982) The jackknife, the bootstrap and other resampling plans. Philadelphia, Penn.: Society for Industrial and Applied Mathematics

Embrapa (Empresa Brasileira de Pesquisa Agropecuária) (1988) Zoneamento ecológico para plantios florestais no estado de Santa Catarina. Curitiba, Brazil. https://ainfo.cnptia.embrapa.br/digital/bitstream/item/17024/1/doc21.pdf Acessed 25 June 2022

Hakamada RE, Stape JL, de Lemos CCZ, Almeida AEA, Silva LF (2015) Uniformidade entre árvores durante uma rotação e sua relação com a produtividade em *Eucalyptus* clonais. Cerne 21 (3): 465–472. https://doi.org/10.1590/01047760201521031716

Hall KB, Stape JL, Bullock BP, Frederick D, Wright J, Scolforo HF, Cook R (2019) A growth and yield model for *Eucalyptus benthamii* in the Southeastern United States. For. Sci. 66 (1): 25-37. https://doi.org/10.1093/forsci/fxz061

IBÁ (Indústria Brasileira de Árvores) (2022). Annual report of IBÁ 2022, base year 2021. https://www.iba.org/datafiles/publicacoes/relatorios/relatorioiba2021-compactado.pdf Accessed 30 November 2022

Lam TY, Guan BT (2020) Modeling stand basal area growth of *Cryptomeria japonica* D. Don under different planting densities in Taiwan. J. For. Res. 25 (3): 174-182. https://doi.org/10.1080/13416979.2020.1733171

McTague JP, Bailey RL (1987). Compatible basal area and diameter distribution models for thinned loblolly pine plantations in Santa Catarina, Brazil. For. Sci. 33(1): 43–51. https://doi.org/10.1093/forestscience/33.1.43

McTague JP, Patton DR (1989) Stand density index and its application in describing wildlife habitat. Wildl. Soc. Bull. 17(1): 58–62.

McTague JP, O'Loughlin D, Roise JP, Robison DJ, Kellison RC (2008) The SOHARC model system for growth and yield of southern hardwoods. South. J. Appl. For. 32 (4): 173–183. https://doi.org/10.1093/sjaf/32.4.173

Montes CR (2012) A resource driven growth and yield model for loblolly pine plantations. PhD Dissertation, North Carolina State University.

Oliveira LC (2012) Erosão hídrica e alguns processos hidrológicos em plantios de pinus, mata, campo nativo e estrada florestal.PhD Thesis Federal University of Santa Catarina.

Peng C (2000) Growth and yield models for uneven-aged stands: past, present and future. For. Ecol. Manage. 132: 259–279. https://doi.org/10.1016/S0378-1127(99)00229-7

Pienaar LV, Shiver BD (1986) Basal area prediction and projection equations for pine plantations. For. Sci. 32 (3): 626-633. https://doi.org/10.1093/forestscience/32.3.626

R Core Team (2019) R: A language and environment for statistical computing. R Foundation for Statistical Computing, Vienna. http://www.R-project.org Accessed 09 November 2020)

Retslaff FAS, Figueiredo Filho A, Machado SA, Arce JE, Jaskiu E (2016) Diagrama de manejo da densidade para *Pinus taeda* no estado do Paraná. Floresta 46 (2): 185-195. https://doi.org/10.5380/rf.v46i2.38301

Ryan MG, Stape JL, Binkley D, Fonseca S, Loos RA, Takahashi EN, Silva CR, Silva SR, Hakamada RE, Ferreira JM, Lima AMN, Gava JL, Leite FP, Andrade HB, Alves JM, Silva GGC (2010) Factors controlling Eucalyptus productivity: how resource availability and stand structure alter production and carbon allocation. For. Ecol. Manage. 259: 1695–1703. https://doi.org/10.1016/j.foreco.2010.01.013

Santos GM, Oliveira XM, Homczinski I, Mayrinck RC, Cavassim WS (2021) Generalized mixed modeling to estimate tapering of *Pinus taeda* trees in different planting spacings. Adv. For. Sci. 8 (1): 1261-1269. http://dx.doi.org/10.34062/afs.v8i1.12414

Schneider PSP, Finger CAG, Schneider PR, Mendes JO (2018) Trajetória bioeconômica dos regimes de manejo em povoamentos de *Pinus taeda* L. Ci. Flor. 28 (3): 1104-1117. https://doi.org/10.5902/1980509833357

Scolforo HF, McTague JP, Burkhart H, Roise J, Campoe OC, Stape JL (2019a) Eucalyptus growth and yield system: Linking individual-tree and stand-level growth models in clonal Eucalypt plantations in Brazil. For. Ecol. Manage. 432, 1–16. https://doi.org/10.1016/j.foreco.2018.08.045

Scolforo HF, McTague JP, Burkhart H, Roise J, McCarter J, Alvares CA, Stape JL (2019b) Stand-level growth and yield model system for clonal eucalypt plantations in Brazil that accounts for water availability. For. Ecol. Manage. 448: 22–33. https://doi.org/10.1016/j.foreco.2019.06.006

Scolforo HF, McTague JP, Raimundo MR, Weiskittel A, Carrero O, Scolforo JRS (2018) Comparison of taper functions applied to eucalypts of varying genetics in Brazil: Application and evaluation of the penalized mixed spline approach. Can. J. For. Res. 1: cjfr-2017-0366. https://doi.org/10.1139/cjfr-2017-0366

Sun H, Zhang J, Duan A, He C (2007) A review of stand basal area growth models. For. Stud. China 9 (1): 85-94.https://doi.org/10.1007/s11632-007-0014-2

Sun HG, Diao S, Liu R, Forrester D, Soares A, Saito D, Dong R, Jianga J (2018) Relationship between size inequality and stand productivity is modified by self-thinning, age, site and planting density in Sassafras tzumu plantations in central China. For. Ecol. Manage. 422: 199–206. https://doi.org/10.1016/j.foreco.2018.02.003

Trilleras AB, Aguirre AML (2020) Basal area growth models for *Eucalyptus tereticornis* Smith stands on the Colombian Atlantic coast. Madera y Bosques 26(2): e2621924. https://doi.org/10.21829/myb.2020.2621924

Vanclay JK (1994) Modelling Forest Growth and Yield: Applications to Mixed Tropical Forests. Wallingford, U.K: CAB International.

Weiskittel AR, Hann DW, Kershaw Jr JA, Vanclay JK (2011) Forest Growth and Yield Modeling. 1. ed. Oxford: John Wiley & Sons.

Wickham H (2016) ggplot2: Elegant Graphics for Data Analysis. Springer, New York. https://cran.r-project.org/web/packages/ggplot2/index.html Accessed 10 November 2020.

Xu Y, Goodacre R (2018) On splitting training and validation set: a comparative study of cross-validation, bootstrap and systematic sampling for estimating the generalization performance of supervised learning. J. Anal. Test. 2(3): 249-262. https://doi.org/10.1007/s41664-018-0068-2